Fracture of elastomers under static mixed mode: the strain energy density factor

Adel Hamdi, Nourredine Aït Hocine, Moussa Nait-Abdelaziz, Noureddine Benseddiq

Fracture of elastomers under static mixed mode: the strain-energy-density factor

A. Hamdi, N. Aït Hocine, M. Naït Abdelaziz, N. Benseddiq

Abstract This work deals with the fracture of rubbers under a mixed mode loading (I+II) and it is an extension of our previous papers on that subject [Aït Hocine N, Naït Abdelaziz M, Imad A (2002) Int J Fract 117:1–23; Aït Hocine N, Naït Abdelaziz M (2004) In: Sih GC, Kermanidis B, Pantelakis G (eds) 6th international conference for mesomechanics. Patras (Greece), May 31–June 4, pp 381–385]. An experimental and a numerical analysis were carried out using a Styrene Butadiene Rubber (SBR) filled with 20 and 30% of carbon black. Sheets with an initial central crack (CCT specimens) inclined with a given angle compared to the loading direction were used. The J-integral and its critical values J_c (fracture surface energy) were determined by combining experimental data and finite element results. These critical values, determined at the onset of crack growth, were found to be quite constant for each elastomer tested, which suggests that J_c represents a reasonable fracture criterion of such materials. Then, the strain–stress field and the strain-energy-density factor S, earlier introduced by Sih [Sih GC (1974) Int J Fract 10(3):305–321; Sih GC (1991) Mechanics of fracture initiation and propagation. Kluwer Academic Publishers, Dordrecht, 428 pp] were numerically calculated around the crack tip. According to the experimental observations, the plan of crack propagation is perpendicular to the direction of the maximum principal stretch. Moreover, as suggested by Sih in the framework of linear elastic fracture mechanics (LEFM), the minimum values $S^{\min}$ of the factor S are reached at the points corresponding to the crack propagation direction. These results suggest that the concept of the maximum principal stretch and the one of the strain-energy-density factor can be used as indicators of the crack propagation direction.

Keywords Rubber · J-integral · Strain-energy-density factor · Fracture criterion · Crack propagation direction

A. Hamdi · M. Naït Abdelaziz · N. Benseddiq
LML, UMR CNRS 8107, Polytech'Lille,
avenue P. Langevin, 59655 Villeneuve-in Ascq, France

N. Aït Hocine (✉)
Laboratoire de Rhéologie, Université de Bretagne Occidentale, 6 avenue Victor Le Gorgeu, C.S. 93837, 29238 Brest, France
e-mail: nourredine.aithocine@univ-brest.fr

1 Introduction

Generally speaking, two general approaches are available when dealing with the fracture of rubbers. The first one is based on the works of Griffith (1920, 1924) which originated more than 80 years ago. Since the energy balance is written for the whole specimen, the knowledge of the stress and strain distribution, especially around the crack tip, is not required. This energy balance leads to the definition of a parameter, called J and representing the energy needed to extend the pre-existing defect of a unit area A:

$$J = -\left.\frac{dU}{dA}\right|_u \tag{1}$$

In relation (1), U is the potential strain energy (equivalent to the area under the load–displacement curve issued from the uniaxial tensile test). The suffix u indicates that derivation is taken under a constant displacement. The parameter J given by Eq. 1 is equivalent to the well-known J-integral initially introduced by Cherepanov (1967) and Rice (1968) in the case of small deformations:

$$J = \int_{\Gamma} \left(W dx_2 - \vec{t}\,\frac{\partial \vec{u}}{\partial x_1} ds \right) \tag{2}$$

where W denotes the strain energy density, (x_1, x_2) is an orthogonal co-ordinate system with x_1-axis parallel to the notch surface, Γ is a curve surrounding the notch tip, ds is a small element of Γ, $\vec{t}$ is the traction vector related to the Cauchy stress tensor components σ_{ij} by $t_i = \sigma_{ij} \cdot n_j$ ($i = 1, 2$ and $j = 1, 2$), $\vec{u}$ is the displacement vector and $\vec{n}$ is the outward normal on Γ. The integral assumes the same value for all paths Γ surrounding the crack tip. Although Rice's proof was given in the context of infinitesimal deformations with linear or non-linear stress–strain relationships, the same conclusions hold true for finite deformations (Knowles and Sternberg 1972; Wang 1973; Oh 1976; Chang and Gao 1997). In the latter case, the J-integral of Rice may still be written in the form of Eq. 2 (Wang 1973; Oh 1976; Chang and Gao 1997) provided that W represents the strain energy density per unit initial volume, $\vec{t}$ is nominal traction vector, σ_{ij} are contravariant components of the stress tensor resolved with respect to the initial base vectors $(\vec{x}_1, \vec{x}_2)$ and referring to the undeformed geometry, x_1 and x_2 are the initial cartesian co-ordinates, and ds is the differential arc length along Γ defined in the undeformed state.

Hence, crack growth will start at some critical value J_c of J. This value should be an intrinsic property of the material, i.e. it should be independent of the crack geometry and the loading. The widely used crack initiation criterion in rubbers is the tearing energy concept introduced by Rivlin and Thomas (1953). This criterion represents an extension of Griffith's (1920, 1924) approach initially developed in the case of the linear elastic framework. It is also equivalent to the energy rate interpretation of the J-integral given by relation (1) (Rice 1968). Unfortunately, such a criterion is not able to predict the propagation direction of a crack. In this case, strain and stress fields or their combination can represent good alternative approaches that were originally developed to study the fracture of metallic materials.

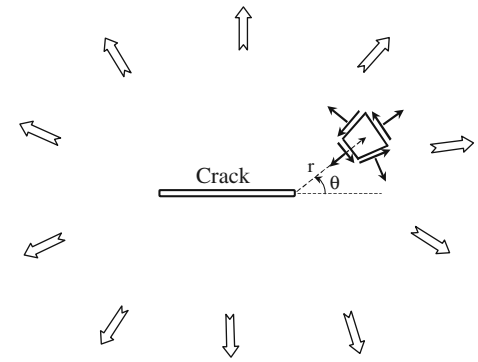

Fig. 1 Crack in general stress field

Dealing with linear elastic mechanical behaviour, Sih (1974, 1991) theoretically analysed the strain-energy-density field near the crack tip under multiaxial loading (Fig. 1). Since the singularity in the strain-energy-density is of the form $1/r$, he defined an energy parameter S, named "the strain-energy-density factor" written as:

$$S = W \cdot r \tag{3}$$

where W is the strain-energy-density and r is a fixed radial distance measured from the crack tip (Fig. 1). r should be small compared with the crack length. Then, he postulated that:

- the initial crack growth takes place in the direction along which the strain-energy-density factor exhibits a stationary (minimum $S^{\min}$) value, i.e. $\frac{\partial S}{\partial \theta} = 0$ at which $\theta = \theta_0$ with $-\pi < \theta_0 < +\pi$.
- the critical value $S_c^{\min}$ of $S^{\min}$ could represent a fracture toughness measure of the material.

Indeed, r being constant, an initial crack will propagate in the direction which requires the least energy, that means a minimum value $S^{\min}$ of S.

The series of experiments that he performed on Plexiglas materials confirmed his theoretical predictions. Moreover, in the last decade, this mesoscopic approach has been successfully extended to other kinds of materials (Yue et al. 1997; Liang et al. 2000; Zheng et al. 2001; Sih 2004). However, to date it has never been

applied in the case of finite deformations except in our recent work (Aït Hocine et al. 2004) dealing with the fracture of rubbers under mode (I) loading. Double edge notch in tension (DENT) specimens with various crack lengths were experimentally tested and a finite element (FE) analysis was performed. The results obtained particularly highlighted that the critical value S_c of the strain-energy-density factor S seems to govern the crack initiation in elastomers according to the analysis of such specimens submitted to mode (I) loading.

In the present study, we try to verify if this concept can be extended to very highly deformable materials under a mixed mode (I+II). This combined loading was assumed to be induced around the crack tip by using sheets containing a central crack inclined with a given angle regarding the uniaxial loading direction.

2 Experimental study

2.1 Materials, specimens, tests

The experiments were carried out using a Styrene Butadiene Rubber (SBR) filled with carbon black in the proportions of 20% (SBR1) and 30% (SBR2). Such synthetic elastomers show substantially non-linear reversible elasticity and display large deformations.

The constitutive law is identified from the engineering stress–strain relationship that is provided by tensile tests performed on an Instron device on three rectangular unnotched sheets of 2 mm thickness, 30 mm length and 6 mm width. The load cell measurements allow the computation of the engineering stress by dividing the applied load by the original area of the specimen cross section. Corresponding engineering strains are deduced from the elongation measured with a CCD camera that follows the changes in the distance l_0 between two circle marks printed on the surface of the specimen (Fig. 2). Data measurements are recorded using a computer which is connected to the experimental setup.

Fracture tests were performed using specimens containing an inclined central crack introduced by a razor blade. The dimensions of these specimens are: length $h = 116$ mm, width $w = 70$ mm and thickness $B = 2$ mm (Fig. 3). The considered crack length is $a = 38.5$ mm with four orientations defined by the angle $\alpha = \{0°, 15°, 30°, 45°\}$. Specimens were loaded in a uniaxial

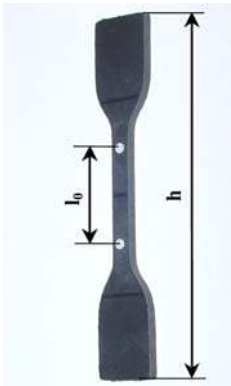

Fig. 2 Specimen geometry used for the identification of constitutive law constants

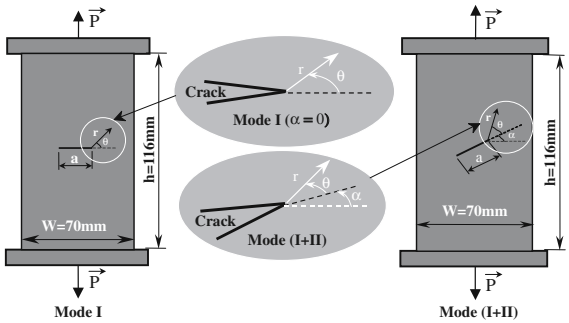

Fig. 3 Geometry of the centre cracked specimens used in fracture tests

direction but a mixed mode (I+II) could be induced around the crack tip because of the crack inclination.

An out plane displacement was observed at the free edge of the crack, but it was significant only at high stretches.

Loads versus displacements were recorded up to total breaking. The maximum global stretches λ_c at crack initiation were noted using an LCD camera that screens on a computer the moving picture of the crack tip zone. The obtained values are reported in Table 1. The recorded images clearly show that a pre-existing notch always propagates perpendicularly to the loading direction (Fig. 4), whatever the initial crack orientation is.

2.2 Constitutive law

The mechanical behaviour of rubbers is commonly described using a hyperelastic formalism leading to the expressions of the strain-energy-density W defined in terms of the strain invariants (Oden 1972). Cauchy stresses as a function of stretches can then be derived from the function W.

Table 1 Maximum global stretches λ_c at crack initiation

Angle $\alpha(^\circ)$	Maximum global stretches λ_c	
	SBR1	SBR2
0	1.36	1.41
15	1.41	1.45
30	1.49	1.53
45	1.65	1.69

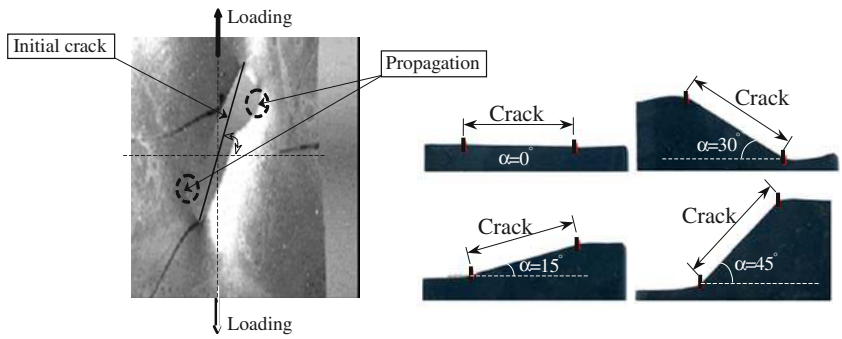

Fig. 4 Initiation and propagation of a pre-existing crack in rubbers studied. (**a**) Crack initiation (initial crack orientation $\alpha = 45°$); (**b**) total breaking

a) Crack initiation (initial crack orientation $\alpha = 45°$) **b)** Total breaking

Table 2 Material constants

Material	C_{10} (MPa)	C_{20} (MPa)	C_{30} (MPa)	C_{01} (MPa)	C_{02} (MPa)
SBR1	2.17×10^{-1}	3.96×10^{-2}	9.06×10^{-4}	4.33×10^{-2}	2.40×10^{-2}
	C_{03} (MPa)	C_{11} (MPa)	C_{12} (MPa)	C_{21} (MPa)	
	3.11×10^{-7}	-4.83×10^{-2}	-1.49×10^{-5}	-5.73×10^{-3}	
SBR2	C_{10} (MPa)	C_{20} (MPa)	C_{01} (MPa)	C_{02} (MPa)	C_{11} (MPa)
	3.76×10^{-1}	1.27×10^{-2}	1.14×10^{-2}	2.11×10^{-5}	3.81×10^{-4}

Identification of the constitutive law parameters requires both uniaxial and biaxial loading experimental data. Since only uniaxial experimental data are available, a theoretical response under biaxial loading is built using the method introduced by Lambert-Diani (1999). This method is based on the fact that for a given experimental uniaxial strain ε_{uni} corresponding to a stress σ_{uni}, an equivalent equibiaxial deformation $\varepsilon_{\text{bia}}^{\text{eq}}$ exists corresponding to the same stress $\sigma_{\text{bia}}^{\text{eq}} = \sigma_{\text{uni}}$.

Fitting experimental uniaxial and theoretical biaxial engineering stress–strain curves leads to identifying the model that best describes the mechanical behaviour of our materials. The constitutive laws of the SBR1 and the SBR2 seem to follow, with the assumption of a nearly incompressibility condition, the Mooney–Rivlin (1948) model with, respectively, 9 and 5 parameters:

$$W = \sum_{i=0}^{m} \sum_{j=0}^{n} C_{ij} (I_1 - 3)^i (I_2 - 3)^j; \;\; C_{00} = 0 \qquad (4)$$

where C_{ij} are the material constants, I_1 and I_2 are the first and the second invariants of Cauchy Green's right deformation tensor and $\lambda_i = 1 + \varepsilon_i$ are the principal elongations (ε_i being engineering strains).

Material parameter values were evaluated by fitting available data (Table 2) and were used to analytically calculate the engineering stresses and strains that were then compared to experimental uniaxial and theoretical biaxial data. A good agreement is observed for the two materials studied, as illustrated in Fig. 5. Moreover, it must be noted that, beyond the limit of the experimental measure field, predicted stresses continually increase

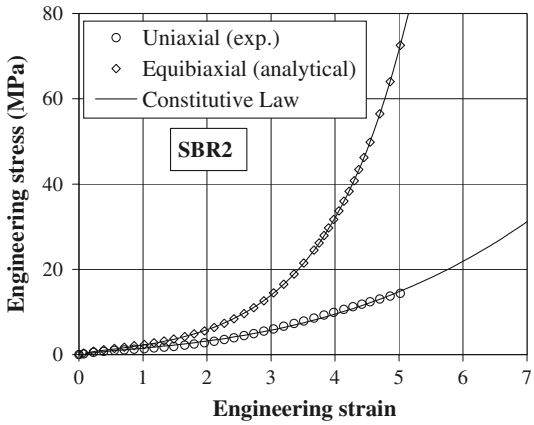

Fig. 5 Engineering stress–strain evolution of the material

with the stretch λ, which ensures that the convergence of the finite element calculations will not be hobbled.

3 Finite elements study

3.1 Model and meshing

All the above mentioned fracture tests were numerically simulated using the finite elements (FE) program "Ansys". The whole sheet was modelled except when the crack was perpendicular to the loading direction ($\alpha = 0°$) where, according to symmetries, only a quarter of the specimen was considered. The crack tip is not sharp and exhibits a curvature radius of 0.1 mm, which corresponds to approximately half of the razor blade thickness. Introducing such a radius avoids the meshing distortion at the vicinity of the crack tip under high deformations. Figure 6 shows, as an example, a selected meshing for a sample with the initial crack orientation $\alpha = 30°$. This meshing contains only quadrilateral elements with eight nodes for the whole specimen and is refined in the vicinity of the crack tip. In this zone, the semi-circle representing the crack notch is subdivided into 24 equal segments. According to this division, the dimensions of first raw of the elements surrounding the crack tip are $0.013 \times 0.34\,\text{mm}^2$. Plane stress and large strains were assumed in the analysis.

The FE calculation was achieved by gradually increasing the displacements applied to the nodes located at the top of the specimen, with equilibrium iteration at each step (full Newton–Raphson method).

4 Results and discussion

Below we shall discuss the ability of the following parameters:

– the J-integral,

– the principal stretches and stresses,

– the strain-energy-density (SED) factor,

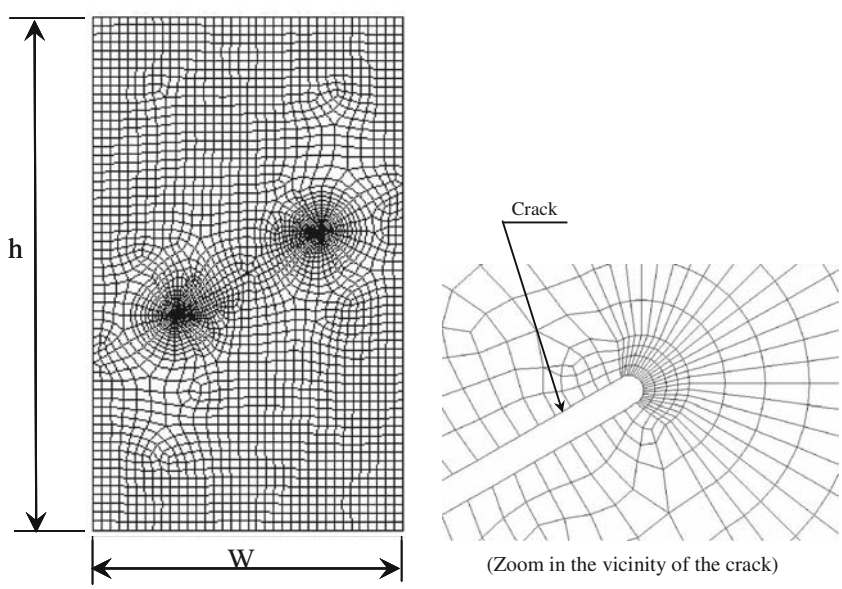

Fig. 6 Example of a selected meshing ($\alpha = 30°$)

to be used as fracture criteria and/or indicators of the crack propagation direction in rubbers. Only selected examples are shown when the results exhibit the same trends for all other configurations studied.

4.1 J-Integral

The J-integral is computed using Eq. 2, considering finite deformations, through three different contours surrounding the crack tip (Fig. 7). Each contour Γ intersects elements of gridwork at a series of points required for the numerical interpolation. Bekker (1983) suggested the contour element intersection should pass through the integration points so as to avoid such further interpolation and this is ideally suited for accurate calculation of the strain-energy-density W.

The path independence of the J-integral is clearly illustrated in Fig. 8 as an example for a particular initial crack orientation. This property was verified for all configurations studied and the slight difference pointed out is less than 0.5%.

The critical values of J corresponding to the crack initiation are reported in Fig. 9 as a function of the initial crack orientation α. This graph clearly shows that the critical values J_c are quite independent of the angle α for the two materials studied with a maximal discrepancy of about 4%. This result means that J_c could also represent, as previously observed for the mode (I) loading (Aït Hocine et al. 2002), a fracture criterion of rubbers under mixed mode. However, J-parameter cannot predict the crack propagation direction. So, which local parameter is able to achieve it in the case of rubbers?

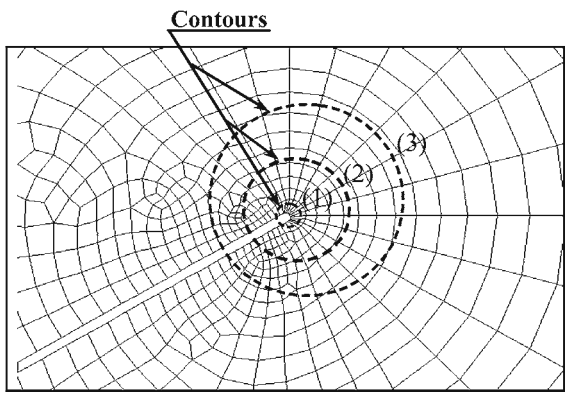

Fig. 7 Contours delimiting some elements used for the J-integral evaluation

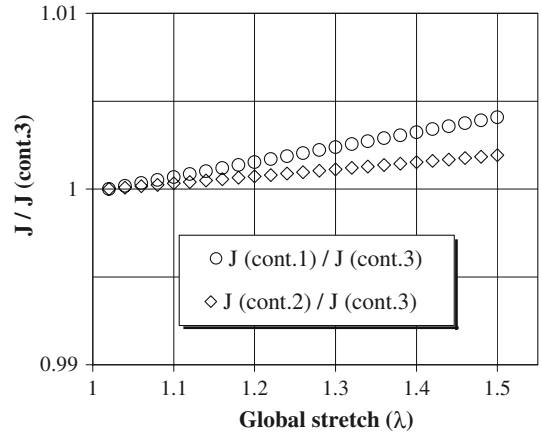

Fig. 8 Influence of the contour position on the J-integral values ($\alpha = 30°$)

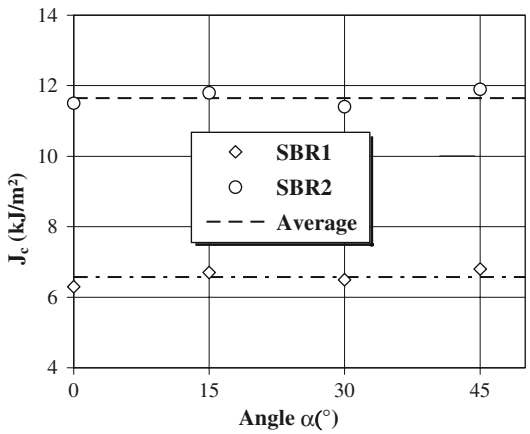

Fig. 9 Numerical fracture energy J_c as a function of the initial crack orientation α

The analyses of some local parameters such as principal stretches, principal stresses or SED factor may give an adequate answer.

4.2 Principal stretches and principal stresses

The maximum principal stretch criterion was introduced by Cadwell et al. in 1940 as a fracture criterion in rubbers containing no defects. Moreover, it was experimentally observed that the crack nucleation plane or the propagation direction of a pre-existing defect is perpendicular to the maximum principal stretch. In fact, strain is a natural choice because it can be linked to the maximum stretch which can be supported by a molecular chain (Gent 2004; Kakavas and Blatz 2005).

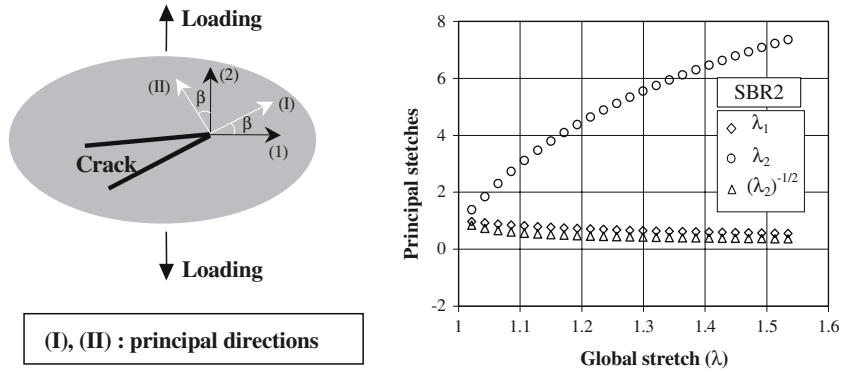

Fig. 10 Evolution of the principal elongations as a function of the stretch λ (SBR2, $\alpha = 30°$)

The F.E. analyses allow the calculation of the Green-Lagrange strain tensor ($\overline{\overline{E}}$) components. These values were computed at the node located in the middle of the semi-circle representing the notch tip. Characteristics of the selected meshing are given in Sect. 3.1. The principal stretches were then obtained according to the following relationship:

$$\overline{\overline{E}} = \frac{1}{2}(\overline{\overline{C}} - \overline{\overline{I}}) \tag{5}$$

where $\overline{\overline{C}} = \overline{\overline{F}}^T \overline{\overline{F}}$ and $\overline{\overline{I}}$ is the unit tensor, $\overline{\overline{F}}$ being the deformation gradient tensor.

The principal directions (I, II, III) were analytically determined and they refer to the undeformed geometry since the used strain tensor measurements are purely Lagrangian. In these principal directions, Eq. 5 becomes:

$$E_i = \frac{1}{2}(\lambda_i^2 - 1),\ i = \{1, 2, 3\} \text{ since } \overline{\overline{F}} = \begin{bmatrix} \lambda_1 & 0 & 0 \\ 0 & \lambda_2 & 0 \\ 0 & 0 & \lambda_3 \end{bmatrix}. \tag{6}$$

It appears that the principal directions (I, II) coincide with horizontal and vertical directions (1, 2) independently of the loading level (Fig. 10). Indeed, it was found that the angle β indicating the orientation of a principal direction regarding the horizontal axis is equal to zero no matter what both the applied stretch value and the crack orientation α were. The evolution of the two principal stretches is plotted in Fig. 10. It highlights that the principal elongation λ_1 is negligible in comparison to λ_2 independently of the loading level. Although it is only shown for a typical example, all the results obtained exhibit the same trends. The criterion of crack propagation direction based upon the maximum principal stretch is in good agreement with the experimental observations since it always predicts a horizontal direction.

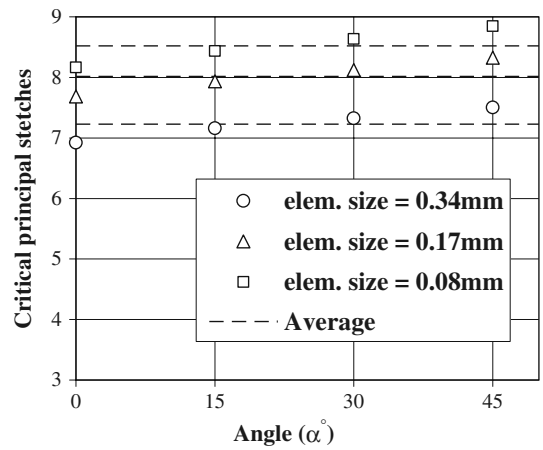

Fig. 11 Critical principal elongations λ_2 as a function of the angle "α"

One may notice that the strain state at the crack tip is closer to that of uniaxial tension (Fig. 10) since in this case: $\lambda_1 \approx 1/\sqrt{\lambda_2}$. Indeed, under the incompressibility assumption, the deformation gradient tensor is expressed as:

$$\overline{\overline{F}} = \begin{bmatrix} \lambda^{-1/2} & 0 & 0 \\ 0 & \lambda & 0 \\ 0 & 0 & \lambda^{-1/2} \end{bmatrix} \tag{7}$$

Moreover, as shown in Fig. 11, the critical values of the principal stretches corresponding to crack initiation, seem to be quite independent of the crack orientation even they slightly increase with α. Indeed, the values exhibit a scattering of about $\pm 4\%$. One may conclude that this quantity is a good candidate for a fracture criterion parameter of such materials.

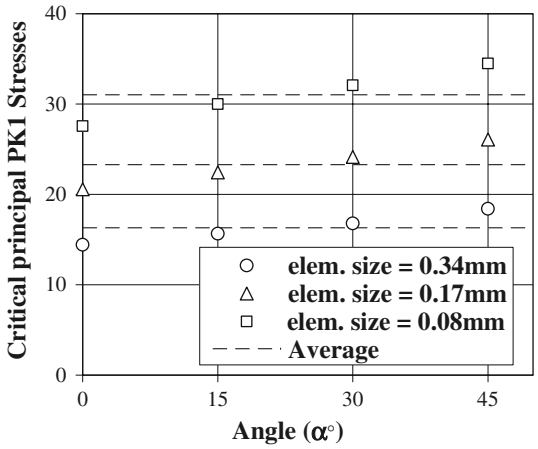

Fig. 12 Critical principal PK1 stresses as a function of the angle "α"

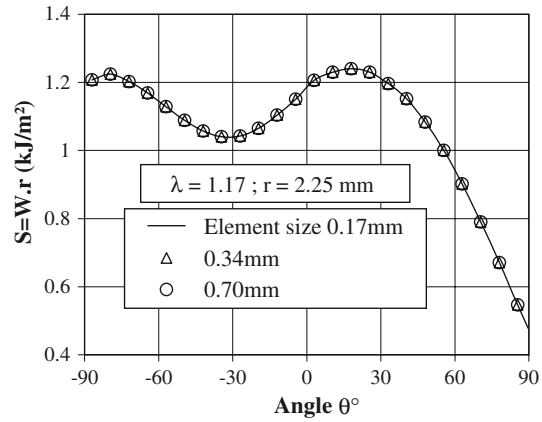

Fig. 13 Influence of meshing on the evolution of the SED factor ($\alpha = 30°$)

The same analysis was achieved by examining the principal first Piola-Kirchhoff (PK1) stresses which is the conjugate of $\overline{\overline{F}}$. The evolution of its critical principal values as function of α is shown in Fig. 12. The dependence on α is here more accentuated. The scattering around an average value is of about $\pm 12\%$. This divergence is higher than that obtained for λ because of the extreme hardening of the material when approaching failure (a small increase of the strain leads to an important drop of the stress).

So, the crack initiation criterion based upon the maximum principal stretches is more relevant than the one provided by the first Piola-Kirchhoff stress values.

Three kinds of mesh refinements in the vicinity of the crack tip were used to examine the influence of the element size on the strain and stress values. As expected, the smaller is the element size, the higher are strains and stresses. However, the critical values of these quantities keep the same trends independently of the meshing type as exhibited by Figs. 11 and 12 for elongations and PK1 stresses, as an example, along the principal direction II.

4.3 Strain-energy-density (SED) factor

The strain-energy-density was evaluated at all nodes and its distribution was analysed in the surrounding crack tip zone. The sensitivity of this quantity to mesh refinement was analysed. As illustrated in Fig. 13 for an angle $\alpha = 30°$ and for a given global stretch $\lambda = 1.17$, the element size has no influence on the SED factor S (relation 3). It must be noted that similar results were obtained for all other initial crack orientations and for all the stretch range up to breaking. Hence, one may conclude that it is reasonable to denote the magnitude of the strain-energy-density W by the SED factor S as was initially proposed by Sih in LEFM framework (Sih 1974, 1991).

Checking the element size of 0.34 mm in the vicinity of the crack, the numerical parameter S was calculated at all nodes surrounding the notch, for different loading levels especially at the onset of the crack growth. The results obtained are shown in Fig. 14 in terms of S as a function of the angle θ (polar co-ordinate) for several assigned values of the radius r. Although, the results reported only concern an SBR2 specimen with initial crack orientation $\alpha = 30°$ and for two given stretches, the same trends were observed for all other cases considered except when the loading is too high. In that case, elements are excessively distorted and the accuracy of the results is no longer ensured.

Figure 14 highlights that, out of a core region surrounding the crack tip (region under complex deformation, i.e. where the nature of deformation is significantly different from those on the outside), the minimum $S^{\min}$ of S is reached at an average angle $\theta = \theta_0$ that remains quite constant independently of the radius r. This angle localises the horizontal direction whatever the initial crack orientation, as illustrated by Fig. 15 for all cases studied, at stretch $\lambda = 1.26$ and for a given radius $r = 5.9$ mm. It must also be noticed that the higher is the loading level, the larger is the core zone. This phenomenon is expected since the factor S cannot

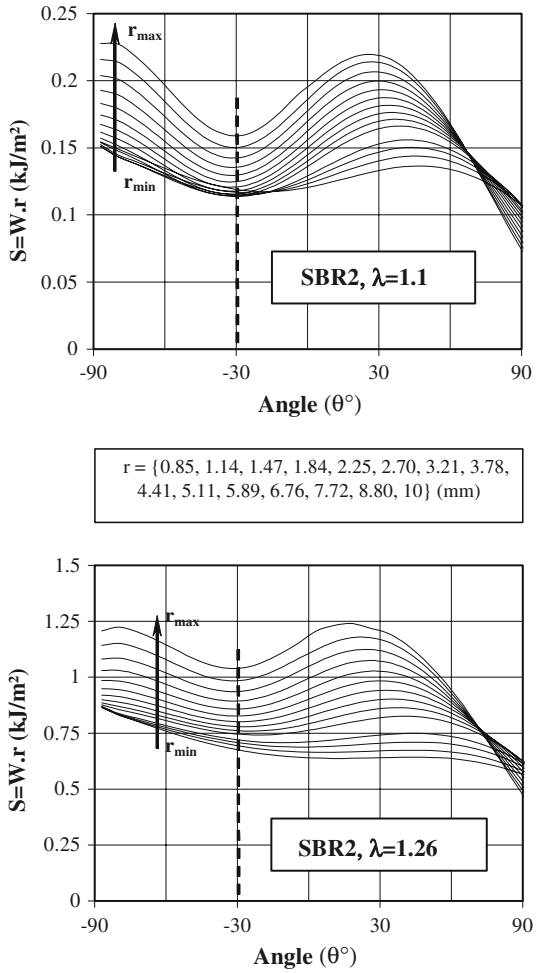

Fig. 14 Evolution of S as a function of θ for several values of the radius r and for two given stretches ($\alpha = 30°$)

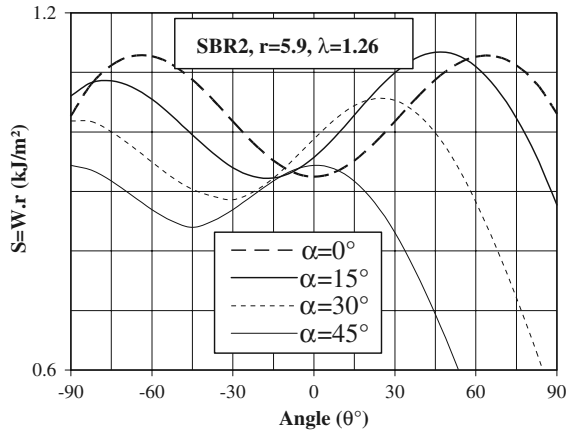

Fig. 15 Evolution of S as a function of θ for a given radius r and stretch λ

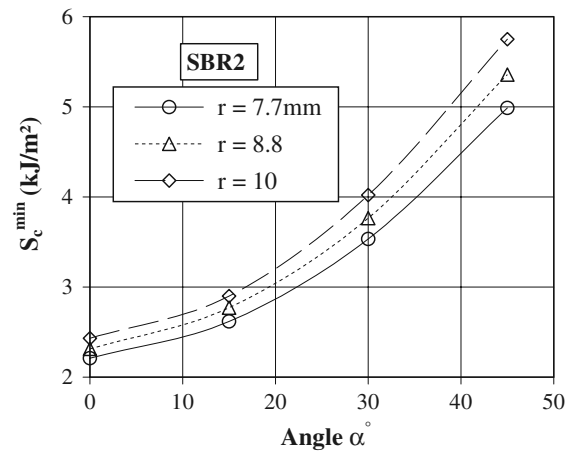

Fig. 16 Critical values $S_c^{\min}$ of the factor S as a function of the initial orientation α of the crack (SBR2)

be accurately evaluated for excessively deformed elements. Nevertheless, the accuracy of FE calculations can be further improved by using an adaptive meshing that consists in mesh regeneration in that zone when the computation is running.

The above numerical results suggest, according to the works of Sih (1974, 1991), that for highly deformable materials under mixed mode (I+II), the crack always propagates perpendicularly to the direction of the loading, independently of the initial crack angle. Such a result is in a good agreement with experimental observations (Fig. 4) and confirms, as already analytically proved by Stephensen (1982), that the mode (I) is always prominent for such materials. This result was also recently confirmed by Martin Borret (1998) who applied an asymptotic method to derive the mechanical stress–strain fields around a crack in rubber components. This work followed the pioneering ones of Wong and Shield (1969) and Knowles and Sternberg (1974).

Finally, the minimum $S_c^{\min}$ of the factor S corresponding to onset of crack growth was evaluated outside the core zone (at $r = \{7.7, 8.8, 10\,\text{mm}\}$) and the values obtained are plotted in Fig. 16 as a function of the initial orientation α of the crack. This graph shows that the critical values $S_c^{\min}$ increase with the angle α indicating that this parameter is not a good candidate to describe the crack initiation.

5 Conclusion

In this work, the fracture of two kinds of rubber-like materials under mixed mode (I+II) was analysed by combining experimental data and FE calculations. Such a loading mode was assumed to be obtained by initially introducing an inclined crack in thin rectangular sheets.

Fracture tests highlighted that, independently of its initial orientation, this pre-existing crack always propagates perpendicularly to the loading direction.

All the experimental tests performed were also numerically simulated using the "Ansys" FE program. The path independence of the J-integral was pointed out in each configuration considered, which confirms the appropriateness of the selected meshing. Moreover, critical values J_c of J corresponding to the crack initiation are quite independent of the initial crack orientation for the two materials studied. This result means that J_c represents a fracture criterion of rubbers under mixed mode (I+II) because for such materials, mode (I) prevails.

To predict the crack propagation direction, an approach based on the maximum principal stretch and stress was examined. It appeared that the maximum principal stretch direction is always perpendicular to the crack propagation plane (horizontal plane). This result suggests that maximum principal stretch is a good indicator of the crack propagation direction in rubber-like materials. In addition, independently of the crack orientation, at the onset of crack initiation, critical principal stretches remain constant, which means that their average value can also be taken as a fracture criterion of such materials.

Finally, the strain-energy-density factor evolution derived for each configuration was analysed. The minimal value of this factor, corresponding to the direction of crack propagation, is always reached in the plan perpendicular to the loading axis, independently of the initial crack orientation. This result is in good agreement with experimental observations. Consequently, the SED factor, developed in the LEFM framework, could be extended to highly non-linear deformable materials as an indicator of the crack propagation direction. However, the critical values $S_c^{\min}$ of S, measured at the onset of crack growth, increase with the angle α suggesting that a fracture criterion based upon a $S_c^{\min}$ value could not be extended to inclined cracks. A relevant fracture criterion could be provided by combining the parameter $S_c^{\min}$ with angle α. This combination must be in adequateness with the results obtained in our previous study dealing with mode (I) loading. Such an analysis is what our future investigations partly aim at.

References

Aït Hocine N, Naït Abdelaziz M, Imad A (2002) Fracture problems of rubbers: J-integral estimation based upon η factors and an investigation on the strain energy density distribution as a local criterion. Int J Fract 117:1–23

Aït Hocine N, Naït Abdelaziz M (2004) Fracture of Rubbers: prediction of the crack propagation direction under mixed mode loading. In: Sih GC, Kermanidis B, Pantelakis G (eds) 6th international conference for mesomechanics, Patras (Greece), May 31–June 4, pp 381–385

Bakker Ad (1983) An analysis of the numerical path dependence of the J-integral. Int J Press Vess Piping 14(3):153–179.

Cadwell SM, Merrill RA, Sloman CM, Yost FL (1940) Dynamic fatigue life of rubber. Ind Eng Chem Anal Ed 12:19–23

Chang JH, Gao YT (1997) Numerical evaluation of J_2-integral for rubbery materials under dynamic loads with finite element method. Comput Mech 20:460–467

Cherepanov GP (1967) The propagation of cracks in a continuous media. J Appl Math Mech 31:503–512

Gent AN (2004) Extensibility of rubber under different types of deformation. J Rheol 49:271–275

Griffith AA (1920) The phenomena of rupture and flow in solids. Phil Trans Roy Soc Lond A 221:163–198

Griffith AA (1924) The theory of rupture. In: Proceeding of the 1st international congress for applied mechanics, pp 55–63

Kakavas PA, Blatz PJ (2005) New constitutive equation for unfilled rubbers based on maximum chain extensibility approch. In: Proceedings of the 4th European conference for constitutive models for rubber, ECCMR, Stockholm, Sweden, 27–29 June

Knowles JK, Sternberg E (1972) On a class of conservation laws in linearized and finite elastostatics. Arch Ration Mech An 44:187–211.

Knowles JK, Sternberg E (1974) Finite-deformation analysis of the elastostatic field near the tip of crack: reconsideration and higher-order results. J Elasticity 4(3):201–233

Lambert-Diani J (1999) Contribution à l' étude du comportement élastique et de l'endommagement des milieux élastomères, thèse (PhD) de l'Ecole Normale Supérieure de Cachan, pp 60–74

Liang W, Shen YP, Zhao M (2000) Magnetoelastic formulation of soft ferromagnetic elastic problems with collinear cracks: energy density fracture criterion. Theor Appl Fract Mech 34:49–60

Martin Borret G (1998) Sur la Propagation de Fissure dans les Elastomères, thèse (PhD) de l'Ecole Polytechnique, Paris, France

Oden JT (1972) Finite elements of nonlinear continua. McGraw-Hill Book Company

Oh HL (1976) A simple method for measuring tearing energy of nicked rubber strips. In: Mechanics of Crack Growth,

American Society for Testing and Materials (ASTM) STP, vol 590, pp 104–114
Rice JR (1968) A path independent integral and the approximate analysis of strain concentration by notches and cracks. J Appl Mech 35:379–386
Rivlin RS (1948) Large elastic deformations of isotropic materials. Phil Trans Roy Soc Lond A 240:459–525
Rivlin RS, Thomas AG (1953) Rupture of rubber. J Polymer Sci 10:291
Sih GC (1974) Strain-energy-density factor applied to mixed mode crack problems. Int J Fract 10(3):305–321
Sih GC (1991) Mechanics of fracture initiation and propagation. Kluwer Academic Publishers, Dordrecht, 428 pp
Sih GC (2004) Fracture mechanics in retrospect in contrast to multiscaling in prospect. In: Proceedings of the 17th national conference of Italian group of fracture, June 16–18, Bologna, pp 15–37
Stephensen RA (1982) The equilibrium field near the tip of crack for finite plane strain of incompressible elastic materials. J Elasticity 10(1):65–99
Wang NM (1973) Finite element analysis of cut growth in sheets of highly elastic materials. Int J Struct 9:1211–1223
Wong FS, Shield RT (1969) Large plane deformations of thin elastic sheets of neo-hookean materials. Zeitschrift Angew Math Phys 20:176–199
Yue ZF, Lu ZZ, Zheng CQ (1997) Fracture behaviour of a nickel-base single crystal superalloy as predicted by the strain-energy-density criterion. Theor Appl Fract Mech 26:89–104
Zheng M, Zhou G, Zacharopoulos DA, Kuna M (2001) Crack behaviour in StE690 characterized by the strain-energy-density criterion. Theor Appl Fract Mech 36:141–145